JOURNAL OF AGRICULTURAL AND FOOD CHEMISTRY

Bioavailability of an Organophosphorus Pesticide, Fenamiphos, Sorbed on an Organo Clay

NEERA SINGH,[†,‡] M. MEGHARAJ,*[,§] W. P. GATES,[‡] G. J. CHURCHMAN,[‡] JENNY ANDERSON,[‡] R. S. KOOKANA,[‡] R. NAIDU,[§] Z. CHEN,[‡] PHIL G. SLADE,[‡] AND N. SETHUNATHAN[‡]

CSIRO Land and Water, PMB 2, Glen Osmond, Adelaide, South Australia 5064, Australia, and Australian Centre for Environmental Risk Assessment and Remediation, University of South Australia, Mawson Lakes, SA 5095, Australia

Hydrolysis of an insecticide/nematicide, fenamiphos [ethyl-3-methyl-4-(methylthio)phenyl-(1-methylethyl)phosphoramidate], immobilized through sorption by cetyltrimethylammonium-exchanged montmorillonite (CTMA−clay) by a soil bacterium, *Brevibacterium* sp., was examined. X-ray diffraction analysis, infrared spectra, and a negative electrophoretic mobility strongly indicated that fenamiphos was intercalated within the bacterially inaccessible interlayer spaces of CTMA−clay. The bacterium hydrolyzed, within 24 h, 82% of the fenamiphos sorbed by the CTMA−clay complex. There was a concomitant accumulation of hydrolysis product, fenamiphos phenol, in nearly stoichiometric amounts. During the same period, in abiotic (uninoculated) controls, 4.6% of the sorbed insecticide was released into the aqueous phase as compared to 6.0% of the sorbed fenamiphos in another abiotic control where activated carbon, a sink for desorbed fenamiphos, was present. Thus, within 24 h, the bacterium hydrolyzed 77% more fenamiphos sorbed by organo clay than the amounts desorbed in abiotic controls. Such rapid degradation of an intercalated pesticide by a bacterium has not been reported before. Evidence indicated that extracellular enzymes produced by the bacterium rapidly hydrolyzed the nondesorbable fenamiphos, even when the enzyme itself was sorbed. Fenamiphos strongly sorbed to an organo clay appears to be readily available for exceptionally rapid degradation by the bacterium.

KEYWORDS: Fenamiphos; organo clay; sorption; bioavailability; hydrolysis

INTRODUCTION

The bioavailability of organic pollutants governs their ecotoxicity and degradation in soils contaminated with them. Even when certain organic pollutants are readily biodegradable and environmental conditions are favorable for their biodegradation, the degradation of pollutants in soils or sediments may be slow or not occur at all. Decreased bioavailability, due to strong sorption by soils, is cited as a major cause for the prolonged persistence of certain biodegradable pesticides in soils (*1*). Generally, only the aqueous phase substrates are readily available for microbial degradation (*2*). The release into solution of soil-sorbed compounds depends on many factors, including the sorption energy of the pesticide molecules, the nature and amount of soil organic matter and clays present, and the soil pH (*1*).

Sorbed compounds have been reported to be available for biodegradation only after their desorption, followed by diffusion into solution (*3*−*5*). Some bacteria can utilize sorbed compounds at rates slightly greater than the rate of the compound's abiotic (uninoculated) desorption from the sorbent (*6*−*9*). In most previous studies, the sorbed substrate was incubated with microorganisms for several days or weeks (*8*); this may have provided sufficient time for its desorption and diffusion into the solution phase. Biosurfactants, produced by microorganisms, as well as synthetic surfactants are able to facilitate desorption of water insoluble compounds, such as phenanthrene. Surfactants promote the solubilization of hydrophobic compounds and also increase their rates of release into solution (*10*). However, there is currently no direct evidence that sorbed compounds are readily available for microbial degradation at sites of sorption, without the compounds being first desorbed into solution.

Organo clay complexes have been used to immobilize organic pollutants, and the biodegradation of pesticides sorbed by modified clays, generally through intercalation, has been the subject of recent interest (*2*, *4*, *5*). In the present study, we determined the bacterial hydrolysis of an organophosphorus insecticide/nematicide, fenamiphos [ethyl-3-methyl-4-(methylthio)phenyl-(1-methylethyl)phosphoramidate], an insecticide used extensively in horticulture and turf greens, that had been immobilized on cetyltrimethylammonium-exchanged montmo-

* To whom correspondence should be addressed. Tel: +61 8 83038703. E-mail: Megharaj.Mallavarapu@unisa.edu.au.
[†] Present address: Division of Agricultural Chemicals, Indian Agricultural Research Institute, New Delhi 110 012, India.
[‡] CSIRO Land and Water.
[§] University of South Australia.

10.1021/jf025978p CCC: $25.00
Published on Web 03/28/2003

Table 1. Desorption of 293.9 nmol of Fenamiphos from CTMA–Clay Complex after Successive Washings with 5 mL of Water

washing sequence	I	II	III	IV
sorbed (nmol)	279.9	268.8	258.1	249.9
desorbed (nmol)	14.0	11.1	10.7	8.11
desorbed (%)	4.78	3.78	3.68	2.76
cumulative desorption (%)	4.78	8.55	12.23	14.97

rillonite (CTMA−Mt). A soil bacterium, *Brevibacterium* sp., was used to demonstrate the hydrolysis of sorbed fenamiphos, which is considered to be a detoxification mechanism (*11*).

MATERIALS AND METHODS

Bacterium, Clay, and Reagents. The bacterium used in this study, *Brevibacterium* sp. (Australian Government Analytical Laboratories Accession Number NM01/22965), capable of readily hydrolyzing fenamiphos (*11*), was isolated from a soil in the Adelaide Hills, near Adelaide, Australia. Fenamiphos (98% pure) and reagent grade CTMA bromide were obtained from Sigma Aldrich, Australia. The clay used was a Na-saturated, <2.0 μm size fraction of Wyoming Mt labeled as "Upton" from American Colloid Corporation (U.S.A.).

Organo Clay (CTMA−Clay) Complex. The CTMA−clay complex was prepared by slow addition of approximately 500 mL of 0.1 M aqueous solution of CTMA bromide to a 1000 mL suspension (0.001 g/mL) of Na−Mt (Na−clay) to exchange all Na. The modified clay was then washed four times with distilled water to remove soluble salts, once with ethanol to remove possible excess CTMA−Br, and dried at 60 °C. X-ray diffraction (XRD) patterns of orientated films of CTMA−clay complex confirmed that adsorption of CTMA in excess of the clay's CEC did not occur (*12*), and analysis by X-ray fluorescence spectroscopy confirmed that excess Br^- had been completely removed.

Fenamiphos-Sorbed CTMA−Clay. Fenamiphos sorption isotherms were conducted by equilibrating 50 mg of CTMA−clay with 5 mL of aqueous solution of fenamiphos in 50 mL Teflon tubes at concentrations of 5, 10, 15, and 20 μg/mL and equilibrated for 24 h. To prepare fenamiphos-sorbed CTMA−clay, fenamiphos, in 5 mL of an aqueous solution (20 μg/mL), 50 mg of CTMA−clay was equilibrated in Teflon tubes (50 mL) for 24 h and the resulting fenamiphos-sorbed organo clay complex was washed four times with 5 mL of distilled water. High-performance liquid chromatography (HPLC) analysis showed that only 15% of the fenamiphos initially sorbed (294 nmol) was released by four successive water extractions (**Table 1**). The 250 nmol of fenamiphos that remained sorbed to CTMA−clay after the final washing was subjected to degradation treatments.

Degradation of Fenamiphos Immobilized on CTMA−Clay. As the goal of this research was to determine the bioavailability of an immobilized insecticide, an incubation period of 24 h, which is short as compared to several days or weeks in previous studies (*8*), was used to minimize the time for desorption or diffusion of the insecticide, if any, from the CTMA−clay. This incubation period was deemed sufficient for equilibrium conditions based on our earlier studies using similar substrate and fenamiphos (data not shown). Fenamiphos (250 nmol), sorbed to 50 mg of CTMA−clay, was suspended in 5 mL of a modified minerals salts medium (*13*) in 50 mL Teflon tubes and then inoculated with a fenamiphos-degrading bacterium (1×10^{10} cells). An uninoculated CTMA−clay suspension with sorbed fenamiphos served as an abiotic control. Another control consisted of CTMA−clay−fenamiphos complex suspended in the uninoculated incubation medium, into which was placed 50 mg of powdered activated carbon enclosed within a molecular porous dialysis membrane (mwco 6000−8000). The activated carbon had a strong affinity for organics and served to sorb any fenamiphos released from the CTMA−clay.

At regular intervals, solution fenamiphos was determined directly by HPLC on the supernatant following centrifugation (6000 rpm for 15 min). Sorbed fenamiphos, as well as the hydrolysis product, fenamiphos phenol (3-methyl-4-methiylthiophenol), were then extracted by dispersing the pellet with 5 mL of methanol and recentrifugation following equilibration of samples on a shaker for 2 h. The supernatant was removed, and the pellet was again dispersed, washed using 5 mL of methanol, equilibrated for another 2 h, and suspension-centrifuged. The supernatant from both extractions was pooled, and the final volume was made to 10 mL for analysis by HPLC.

Degradation by Culture Filtrate. To determine whether the enzyme responsible for hydrolyzing fenamiphos was extracellular, the bacterium was grown on fenamiphos-supplemented tryptone soy broth for 36 h and the cells were removed by filtration through a 0.2 μm Millipore filter. The culture filtrate (5 mL) was then examined for its ability to hydrolyze fenamiphos by adding to 5 mL of mineral salts medium supplemented with fenamiphos at a final concentration of 10 μg/mL. At regular intervals, samples were removed for HPLC analysis.

Influence of CTMA−Clay Components on Enzymatic Activity. We tested whether the CTMA−clay complex or the reagents from which it had formed (Na−clay and CTMA−Br) had any effect on the activity of the crude enzyme. To obtain the crude enzyme, the bacterium was grown on fenamiphos-supplemented tryptone soy broth, and at log phase, the cells were washed twice with 0.2 M phosphate buffer (pH 7.0) by centrifugation (10 000 rpm for 20 min and 4°C) and resuspended in 25 mL of buffer. The cells were then sonified and centrifuged (16 000 rpm for 20 min and 4 °C).

The clarified crude enzyme extract (0.1 mL) was equilibrated separately with 10 mL suspensions (5 g/L) of CTMA−clay complex or Na−clay or 1 g L^{-1} of CTMA−Br solution. After 2 h, centrifugation was used to recover the clay and 1 mL of the supernatant was added to 9 mL of phosphate buffer containing 10 μg fenamiphos/mL. A solution of phosphate buffer without enzyme served as the control. At regular intervals, fenamiphos and fenamiphos phenol concentrations were determined by HPLC in samples removed for analysis.

HPLC. Fenamiphos and its hydrolysis product (fenamiphos phenol) in duplicate samples were extracted in methanol and analyzed using a Varian high-performance liquid chromatograph equipped with a polychrome 9065 diode array detector, an autoinjector, and a 9100 autosampler. Analyses were performed on a reverse phase C_{18} column (Microsorb-MV, 5 μm, 4.6 mm × 250 mm) using an isocratic elution phase of acetonitrile−water (60:40, v/v) and flow rate of 1 mL/min (*11*). UV absorbance at 200 nm was used for detection of fenamiphos or fenamiphos phenol, and peak areas were integrated using Star chromatographic workshop software (Varian) and quantified by comparison with the authentic external fenamiphos standard. Fenamiphos phenol was prepared by hydrolyzing fenamiphos with 0.1 mL NaOH/L at 50 °C for 12 h as described by Ou et al. (*14*). Fenamiphos and fenamiphos phenol were separately identified by cochromatography. Under the conditions used, the retention time was 7.5 min for fenamiphos and 3.5 min for fenamiphos phenol. Recovery of fenamiphos and its phenol by the extraction method used was >80% with a lower quantitative limit of <0.1 μg/g.

XRD. XRD patterns were obtained using a Philips PW1710 diffractometer (Co Kα radiation), fitted with a 0.5° divergence slit, two Soller slits, a graphite monochromator, and a proportional counter. Counting was carried out for 6 s at 0.02° intervals between 2 and 40° 2θ. XRD patterns were collected on the CTMA−clay samples equilibrated with aqueous solutions of fenamiphos as for biodegradation studies (see below) but also on samples equilibrated with much greater concentrations of fenamiphos in ethanol. By assuming that all fenamiphos was sorbed (see Results and Discussion), then, the CTMA−clay complex would contain 0.2, 0.8, 1.5, 2.0, and 3.0 wt % fenamiphos. Following equilibration, samples were prepared as wet pastes in ethanol and dried overnight onto silicon wafers to produce orientated films.

Infrared (IR). IR analysis was conducted on CTMA−clay−fenamiphos samples (0.2 wt % fenamiphos sorbed from aqueous solution) as well as on those samples following biodegradation and control samples prepared to distinguish spectral features. Diffuse reflectance IR Fourier transform (DRIFT) spectra in the mid-IR region were collected (512 scans at 2 cm^{-1} resolution) on washed, dried powders using a Biorad FTS 175C spectrophotometer fitted with an extended KBr beam splitter and a Peltier-cooled solid state (DTGS) detector. The sample compartment was continuously purged with dry, purified, CO_2-free air during analysis. The samples were mixed (approximately 2 wt %) with dry KCl and front-packed into the sample cell. Plane-polarized attenuated total reflectance (ATR) IR spectra in

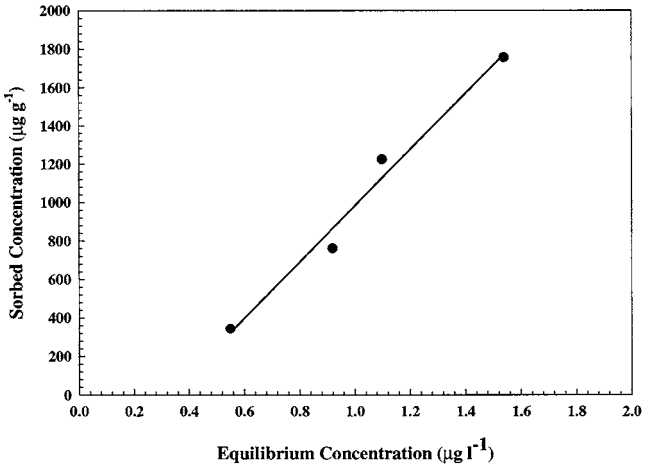

Figure 1. Sorption isotherm of fenamiphos by CTMA–clay.

the mid-IR region were recorded on orientated films of CTMA−clay−fenamiphos complex (0.8 wt % fenamiphos from ethanol solutions) deposited on one side of a ZnSe crystal (45° cleavage). Both the parallel and the perpendicular polarizations were recorded; a parallel polarization results in maximal intensities for dipole transition moments aligned perpendicular to the clay 001 surface; a perpendicular polarization results in minimal intensities for these same dipole transition moments. The curve-fitting program, Grams 32/AI (Galactic), was used to decompose the absorption components in the region of 1750−1350 cm^{-1} in order to estimate the effect of fenamiphos sorption on CTMA and water absorption bands (*15*).

Particle Charge ζ-Potential. Electrophoretic determinations of the ζ-potential were conducted on dilute aqueous suspensions using a Malvern Zetamaster fitted with a ZET5104 general purpose cell. The instrument was previously aligned with a suspension of carboxylated polystyrene latex in a 0.02 M phosphate buffer. The average of five measurements was recorded (with zero-field correction) in the potential range of −100 to 50 mV; each measurement was 20 s in duration. Suspensions were diluted (generally <0.1 mg/mL) such that the photon count rate was within the range of $1.5-2.0 \times 10^6$ counts s^{-1} and the resulting potential width was <3 mV.

RESULTS AND DISCUSSION

Sorption Isotherms. Figure 1 shows the sorption isotherm of fenamiphos from aqueous solutions by CTMA−clay. **Table 1** shows the fenamiphos desorption following successive washes with water. It is clear that considerably less fenamiphos is desorbed than is sorbed for any particular concentration of fenamiphos in solution. Hence, considerable fenamiphos is retained by the organo clay complex against desorption into solution. Strong attraction of fenamiphos by the organo clay is indicated by this result.

Another notable feature of the sorption isotherm is the linear shape, indicating that all sites for interaction between fenamiphos and the sorbent are energetically equivalent. A linear shape arises from a partition mechanism for sorption (*16*). Uptake of nonionic organic molecules by organo clays typically gives a linear isotherm (*17*, *18*), consistent with partitioning of the molecules into the hydrophobic portion of the organic cation intercalated between adjacent aluminosilicate layers. The linear isotherm contrasts with most isotherms for adsorption by solid surfaces, which are typified by changes in sorption rate with solution concentration, often showing a high initial gradient, indicating that higher energy sites are filled first, before adsorption occurs on low energy sites.

Mode of Sorption of Fenamiphos. XRD data (**Figure 2**) showed that fenamiphos is intercalated into the interlayer space of CTMA−clay where it caused the distance between CTMA−clay layers to increase. Greater fenamiphos loadings than were used in the microbial degradation experiments (to confirm intercalation) first resulted in enhanced background intensity at <2−3° 2θ (indicating large *d* spacings) (**Figure 2**, trace C) and then in the appearance of a peak for the CTMA−clay−fenamiphos component with $d(001) \approx 3.5$ nm (**Figure 2**, traces D and E). The 2nd and 3rd orders of this compound overlapped with the *d*(001) of the original CTMA−clay complex. Plots C−E in **Figure 2** show that sufficient sorbed fenamiphos increased the interlayer spacing, demonstrating that fenamiphos entered the interlayer region of the organo clay and caused an expansion of the crystallites. When the complex was loaded with 0.2 wt % sorbed fenamiphos as in the microbial degradation experiments, the main *d*(001) band for CTMA−clay showed a small, although significant, increase from 1.72 (**Figure 2**, trace A) to 1.80 nm (**Figure 2**, trace B) as well as an increase in the full-width at half-maximum (fwhm) of the peak. Because the process of sorption of fenamiphos is continuous with increased solution concentration (**Figure 1**), it appears that intercalation, leading to an increased interlayer spacing, also occurred continuously with fenamiphos addition. Bacterial degradation of this same concentration of sorbed fenamiphos resulted in the return of the *d*(001) to 1.72 nm (not shown).

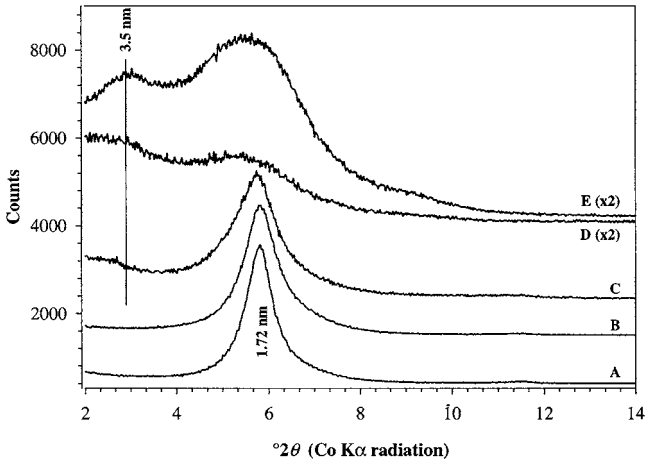

Figure 2. X-ray diffractograms of (**A**) CTMA–clay complex alone; with (**B**) 0.2 wt % sorbed fenamiphos from aqueous solution as in biodegradation studies; and with (**C**) 0.8, (**D**) 2.0, and (**E**) 3.0 wt % sorbed fenamiphos from ethanol solution.

Plane-polarized IR spectra (**Figure 3**) revealed that sorption of fenamiphos by the CTMA−clay complex perturbed both CTMA cations and interlayer water, indicating strong direct interaction between fenamiphos and these two species in the interlayers and providing convincing evidence of fenamiphos intercalation into the interlayer space of CTMA−clay. Although there is overlap between the absorption bands associated with CH_2 scissor for fenamiphos (near 1477 cm^{-1}) (*19*) and that for CTMA (near 1467 cm^{-1}) (**Figure 3**, trace B), fenamiphos sorption was seen to affect the dichroism of other CTMA bands. Decomposition of polarized IR spectra indicated that the dichroism ratio (R_p/R_s) (*15*) for the band near 1487 (parallel asymmetric C−C stretch) increased upon sorption of fenamiphos, while that of the band near 1474 (perpendicular symmetric C−C stretch) decreased (**Table 2**). These transition moment interactions can be interpreted as a rotation of the aliphatic chain symmetry plane with respect to the clay 001 surface upon sorption of fenamiphos (*14*, *20*−*22*). The dichroism ratios of phenyl C−C stretching and deformation bands of fenamiphos all indicated that the ring plane of fenamiphos might reside at a very low angle (<10−20°) with respect to the clay 001

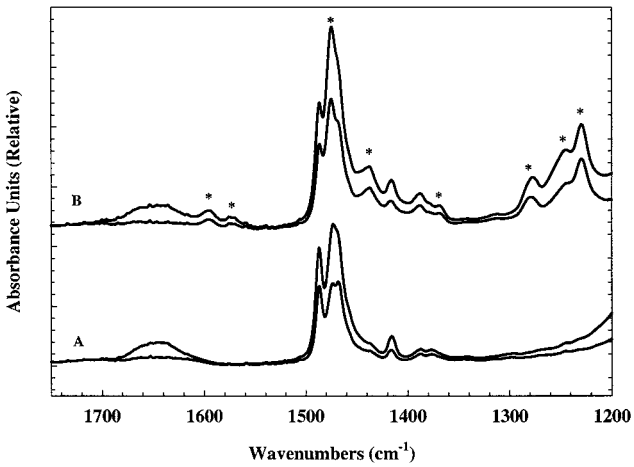

Figure 3. Polarized ATR–IR spectral pairs of (**A**) CTMA–clay alone and with (**B**) 0.8 wt % sorbed fenamiphos. Lower traces in each pair are polarized perpendicular to the incident IR radiation, and the upper traces are polarized parallel to the incident IR radiation. Bands marked with * indicate sorbed fenamiphos. Scale: major tick interval = 0.1 absorbance unit ($A = -\log 1/R$).

Table 2. IR Frequencies, Band Assignments, Dichroic Ratios (R_p/R_s), and Transition Moment Directions with Respect to the Clay 001 Surface for CTMA–MT Complex and CTMA–MT Complex with Sorbed Fenamiphos, as Determined from Polarized ATR

frequency (cm^{-1})	assignment and transition moment	R_p/R_s	moment direction (deg)
	CTMA–MT		
1641	OH bend, cation and surface water	4.5	19
1487	C–C symmetric stretch parallel to chain axis	2.9	22
1474	C–C asymmetric stretch perpindicular to chain axis	6.2	15
1467	symmetric CH_2 scissor perpindicular to chain axis	3.5	21
	CTMA–MT fenamiphos		
1643	OH bend, surface water	1.5	31
1595	phenyl C–C deformation A1 in-ring plane	14.9	10
1572	phenyl C–C deformation B1 in-ring plane	5.1	17
1487	as above	3.3	21
1477	fenamiphos CH_2 scissor perpindicular to chain axis	2.3	24
1474	as above	3.5	21
1467	as above	5.1	17
1416	phenyl C–C deformation B1 in-ring plane	4.1	19
1387	phenyl–S–CH_3 deformation	2.4	25
1367	phenyl–CH_3	1.2	30

surface, as indicated previously (*23*). The absorption band for surface and cation hydration waters near 1645 cm^{-1} in CTMA−clay (**Figure 2**, trace A) broadened considerably, and R_p/R_s decreased upon sorption of fenamiphos. These results indicated that the O−H transition moments of water associated with CTMA cations initially reside at a low angle (∼15−20°) with respect to the clay basal surface and that fenamiphos sorption onto CTMA−clay increases the orientation angle of the O−H transition moment of hydration water. In addition, fenamiphos sorption by CTMA−clay perturbed the H-bonding environment.

Formation of a complex with CTMA hardly affected the charge on the external surface of clay particles, since the

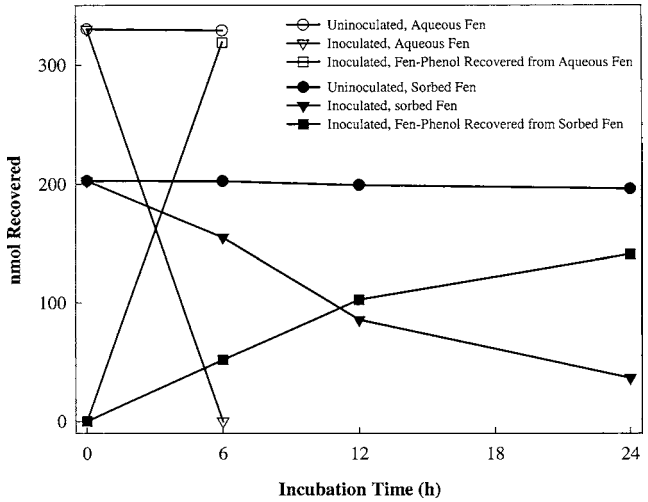

Figure 4. Quantities of fenamiphos recovered from uninoculated aqueous solution (circles); inoculated aqueous solution (inverted triangles); uninoculated suspensions of CTMA–clay complex with 0.2 wt % sorbed fenamiphos (solid circles); and inoculated suspensions of CTMA–clay complex with 0.2 wt % sorbed fenamiphos (solid inverted triamgles). Quantities of the hydrolysis reaction product, Fenamiphos–phenol, recovered from the inoculated aqueous solutions (squares) and inoculated suspensions of CTMA–clay complex with 0.2 wt % fenamiphos (solid squares). Measurement errors are within the dimensions of the symbols. Tests for fenamiphos in aqueous solution were carried out for 6 h only, as trends were obvious.

ζ-potential of the CTMA−clay complex was −45.6, while that of the uncomplexed clay was −49.2. Negative electrophoretic mobility of the CTMA−clay particles used provides evidence that most of the CTMA, at least, is not covering the external surfaces. Xu and Boyd (*24*) also interpreted a negative electrophoretic mobility of a complex of this type as an indication that little of the adsorbed organic cation was located on external surfaces of the clay mineral. The strong interactions between the fenamiphos and the adsorbed cation located in the interlayer of the clay mineral according to sorption isotherms (**Figure 1**, **Table 1**), the XRD evidence (**Figure 2**), and the polarized IR spectra (**Figure 3**, **Table 2**) suggest that fenamiphos is intercalated within the interlayer of the organo clay.

Microbial Degradation of Sorbed Fenamiphos. The bacterium, *Brevibacterium* sp., was able to completely degrade 330 nmol of fenamiphos in a clay-free mineral salt medium within 6 h (**Figure 4**, triangles). Without inoculation, fenamiphos in the same clay-free medium was effectively unchanged over 6 h (**Figure 4**, circles). In a medium containing fenamiphos sorbed by the CTMA−clay complex, 82% of 203 nmol of the insecticide was degraded by the bacterium within 24 h (**Figure 4**, solid triangles). A concomitant and nearly stoichiometric accumulation of fenamiphos phenol occurred in inoculated suspensions containing CTMA−clay complex (**Figure 4**, solid squares). In abiotic (uninoculated) controls, only 3% of fenamiphos sorbed by CTMA−clay was degraded during the same period (**Figure 4**, solid circles). Measurements showed that only 4.6% of sorbed insecticide was released into the aqueous phase, even though the aqueous solubility of fenamiphos is >400 μg/mL.

When reactions were conducted in the presence of activated carbon, only 6.0% of sorbed fenamiphos was desorbed from CTMA−clay complex. This indicates that desorption of the fenamiphos was negligible during 24 h incubation, even though a strong diffusion gradient for desorption was provided by

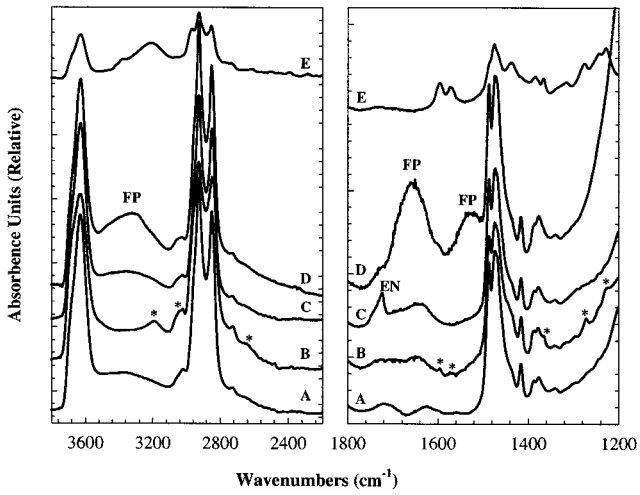

Figure 5. DRIFT-IR spectra of (**A**) CTMA–clay alone and CTMA–clay complexes with (**B**) 0.2 wt % fenamiphos; (**C**) bacterial enzyme extract; and (**D**) the products of **B**, following 24 h reaction with bacteria. (**E**) DRIFT-IR spectrum of a physical mixture of fenamiphos crystals with CTMA–clay. Bands marked with * indicate sorbed fenamiphos, with EN indicating sorbed enzyme and with FP indicating sorbed fenamiphos phenol. Scale: major tick interval = 0.1 absorbance unit ($A = -\log 1/R$).

activated carbon. However, the bacterium was able to hydrolyze 77% more sorbed fenamiphos than could be desorbed in abiotic controls within 24 h. Such rapid degradation of a sorbed pesticide by a bacterium has not been reported before. IR spectra (**Figure 5**) confirmed that the fenamiphos sorbed to the CTMA−clay complex was degraded by the bacterium.

In a recent study by McGhee et al. (*8*), a bacterium, *Pseudomonas* sp., could degrade 58% of 2,4-D sorbed onto an $Al(OH)_x$−Mt (chlorite) complex in 28 days. However, in an abiotic control, around 45% of the sorbed 2,4-D was desorbed into the aqueous phase during this same period. Thus, the bacterium was able to degrade only 13% more 2,4-D than was desorbed abiotically in 28 days. Recently, phenanthrene (a polycyclic aromatic hydrocarbon), intercalated into an organo clay (tetradecyltrimethylammonium−Mt), was shown to be resistant to degradation by bacteria (*25*). Clearly, fenamiphos sorbed by CTMA−clay complex is more bioavailable than phenanthrene intercalated by a similar organo clay. Presumably, structure, size, and aqueous solubility would influence the differences in the degradation of fenamiphos and phenanthrene sorbed to organo clay complexes.

Surfactants of microbial or synthetic origin are known to assist the release of sorbed hydrophobic compounds into solution from soils, sediments, clays, and organo clays; in this way, surfactants can facilitate the biodegradation of the compounds (*1*). The fenamiphos-degrading bacterium used here appears to not produce a surfactant, as there was no measurable change in the surface tension of the growth medium after 4 days of inoculation with the bacterium. A synthetic surfactant, Triton-X100, when added at 10 000 μg mL^{-1}, facilitated desorption of only 10% of fenamiphos from the CTMA−clay complex during 24 h. The fact that even a synthetic surfactant could not readily dislodge the intercalated fenamiphos would indicate the strong sorption of fenamiphos to organo clay.

IR spectra showed that fenamiphos phenol, after its formation by hydrolysis of fenamiphos, remained sorbed to the CTMA−clay complex (**Figure 3**, trace C). Measurements also indicated that the aqueous phase concentration of the breakdown product never exceeded 15% of the sorbed fenamiphos. Probably, fenamiphos was hydrolyzed at the sorbed sites to produce a polar product, which was only partially released into solution.

Evidence for Extracellular Fenamiphos-Degrading Enzyme. Bacterial cells clearly do not have direct access to fenamiphos intercalated into the CTMA−clay complex, because the interlayer space of the CTMA−clay complex (~1.8 nm) is >200 times smaller than the diameter of a typical bacterium (400 nm). We found that viable bacterial cell numbers decreased from 2.0×10^{12} initially to 0.4×10^{7} after 24 h of incubation with suspensions of CTMA−clay. Scanning electron micrographs showed that bacterial cells were attached to the surfaces of organo clay aggregates. We attribute this decrease in viable cells in suspension to their sorption onto the organo clay surfaces. XRD patterns of the CTMA−clay complex showed no perceptible change when the complex was reacted with bacterial cells, indicating that the bacterium had little capability to disrupt the layer spacing of the organo clay. This result also supports the conclusion that the bacterium did not produce a surfactant to disrupt the organo clay. However, bacterial cells on the surfaces of organo clay aggregates, or even in the free state, may degrade the intercalated compound through production of extracellular enzymes. It appears that these enzymes are capable of entering the interlayer space of the organo clay complex, where they can interact with the fenamiphos intercalated therein.

To determine whether the fenamiphos-hydrolyzing enzyme produced by the bacterium was extracellular, the culture filtrate (passed through a 0.2 μm filter) was examined for its ability to hydrolyze fenamiphos. In 24 h, nearly all added fenamiphos (10 μg/mL) was hydrolyzed by the culture filtrate. Extracellular enzymes produced by the bacterium evidently hydrolyzed fenamiphos. Thus, extracellular enzymes produced by the bacterium are probably able to diffuse to the interlayer space of the organo clay complex and hydrolyze the intercalated fenamiphos.

The enzyme added in the free state to fenamiphos solutions or to fenamiphos solutions with Na−clay or CTMA−Br salt readily hydrolyzed fenamiphos. Likewise, the enzyme hydrolyzed fenamiphos after treatment of the CTMA−clay but with less efficiency. Hydrolytic activity of the enzyme was repressed by 50% after equilibration with CTMA−clay, but not by the individual components of the organo clay, as compared to the enzyme in the free state, probably because of sorption of the enzyme by the CTMA−clay complex. Enzyme protein value in the supernatant decreased from 97 to 26 $\mu g/mL^{-1}$ following 2 h of equilibration with CTMA−clay. Interestingly, the CTMA−clay complex with the sorbed enzyme also easily hydrolyzed fenamiphos in solution.

The enzyme produced by the bacterium retains its hydrolytic activity even when sorbed by the CTMA−clay complex. Because bacteria cannot physically penetrate the interlayer spaces of the organo clay, they must access the intercalated nondesorbable pesticide through the production of extracellular enzymes, thereby effecting its exceptionally rapid degradation. Additional evidence for bacterial degradation of nondesorbable fenamiphos is provided by the inability of the bacterium to produce surfactant and the inability of synthetic surfactant or even activated carbon to dislodge the intercalated insecticide from the CTMA−clay complex.

Our results imply that fenamiphos, strongly sorbed by CTMA−clay, by intercalation into its interlayers, is bioavailable because of the (i) rapid bacterial hydrolysis of the intercalated fenamiphos; (ii) little desorption of fenamiphos into the aqueous phase during the reaction time, even in the presence of a

powerful abiotic sink or of a synthetic surfactant; (iii) ability of the bacterium to produce extracellular enzymes that can penetrate the interlayer; and (iv) accumulation of the hydrolysis product mostly on the solid phase.

ACKNOWLEDGMENT

We thank Dr. G. S. R. Krishnamurti (formerly at Saskatoon University, Canada) and Dr. J. M. Bollag (The Pennsylvania State University, U.S.A.) for their critical comments on an initial draft of the manuscript. We are grateful to Mr. S. G. McClure (CSIRO Land and Water) for scanning electron microscopy and Mr. Colin Rivers (Department of Soils and Water, Adelaide University) for help in measuring surface tension of bacterial medium.

LITERATURE CITED

(1) Scow, K. M.; Johnson, C. R. Effect of sorption on biodegradation of soil pollutants. *Adv. Agron.* **1997**, *58*, 1−56.

(2) Xu, S.; Sheng, G.; Boyd, S. A. Use of organoclays in pollution abatement. *Adv. Agron.* **1997**, *59*, 25−62.

(3) Ogram, A. V.; Jessup, R. E.; Ou, L. T.; Rao, P. S. C. Effects of sorption on biological degradation rates of (2,4-dichlorophenoxy)acetic acid in soils. *Appl. Environ. Microbiol.* **1985**, *49*, 582−587.

(4) Guerin, W. F.; Boyd, S. A. Differential bioavailability of soil-sorbed naphthalene to two bacterial species. *Appl. Environ. Microbiol.* **1992**, *58*, 1142−1152.

(5) Crocker, F. H.; Guerin, W. F.; Boyd, S. A. Bioavailability of naphthalene sorbed to cationic surfactant-modified smectite clay. *Environ. Sci. Technol.* **1995**, *29*, 2953−2958.

(6) Tang, W.-C.; White, J. C.; Alexander, M. Utilization of sorbed compounds by microorganisms specially isolated for that purpose. *Appl. Environ. Microbiol.* **1998**, *49*, 117−121.

(7) Calvillo, Y. M.; Alexander, M. Mechanism of microbial utilization of biphenyl sorbed to polyacrylic beads. *Appl. Microbiol. Biotechnol.* **1996**, *45*, 383−390.

(8) McGhee, I.; Sannino, F.; Gianfreda, L.; Burns, R. G. Bioavailability of 2,4-D sorbed to a chlorite-like complex. *Chemosphere* **1999**, *39*, 285−291.

(9) Park, J. H.; Zhao, X..; Voice, T. C. Biodegradation of nondesorbable naphthalene in soils. *Environ. Sci. Technol.* **2001**, *35*, 2734−2740.

(10) Scheibenbogen, K.; Zytner, R. G.; Lee, H.; Trevors, J. T. Enhanced removal of selected hydrocarbons from soil by *Pseudomonas aeruginosa* UG2 biosurfactants and some chemical surfactants. *J. Chem. Technol. Biotechnol.* **1994**, *59*, 53−59.

(11) Megharaj, M.; Singh, N.; Kookana, R. S.; Naidu, R.; Sethunathan, N. Hydrolysis of fenamiphos and its oxidation products by a soil bacterium in pure culture, soil and water. *Appl. Microbiol. Biotechnol.* **2003**, in press.

(12) Rausell-Colom, J. A.; Serratosa, J. M. Reactions of clays with organic substances. In *Chemistry of Clays and Clay Minerals*; Newman, A. C. D., Ed.; Mineralogical Society, Longman Group: Essex, England, 1987; pp 371−422.

(13) Abril, M.-A.; Michan, C.; Timmis, K. N.; Ramos, J. L. Regulator and enzyme specificities of the Tol plasmid-encoded upper pathway for degradation of aromatic hydrocarbons and expansion of the substrate range of the pathway. *J. Bacteriol.* **1989**, *171*, 6782−6790.

(14) Ou, L.-T.; Thomas, J. E.; Dickson, D. W. Degradation of fenamiphos in soil with a history of continuous fenamiphos applications. *Soil Sci. Soc. Am. J.* **1994**, *58*, 1139−1147.

(15) Raupach, M.; Slade, P. G.; Janik, L. J.; Radoslovich, E. W. A polarized infrared and X-ray study of lysine-vermiculite. *Clays Clay Miner.* **1975**, *23*, 181−186.

(16) Chiou, C. T.; Schmedding, D. W.; Manes, M. Partitioning of organic compounds in octanol−water systems. *Environ. Sci. Technol.* **1982**, *16*, 4−10.

(17) Boyd, S. A.; Mortland, M. M.; Chiou, C. T. Sorption characteristics of organic compounds on hexadecyltrimethylammonium-smectite. *Soil Sci. Soc. Am. J.* **1988**, *52*, 652−657.

(18) Jaynes, W. F.; Boyd, S. A. Clay mineral type and organic compound sorption by hexadecyltrimethylammonium-exchanged clays. *Soil Sci. Soc. Am. J.* **1991**, *55*, 43−48.

(19) Farmer, V. C. The layer silicates. In *The Infrared Spectra of Minerals*; Farmer, V. C., Ed.; Mineralogical Society, Longman Group: Essex, England, 1974; Chapter 15, pp 331−363.

(20) Raupach, M.; Janik, L. J. The orientation of ornithine and 6-aminohexanoic acid adsorbed on vermiculite from polarized i.r. ATR spectra. *Clays Clay Miner.* **1976**, *24*, 127−133.

(21) Slade, P. G.; Raupach, M.; Emerson, W. W. The ordering of cetylpyridinium bromide on vermiculite. *Clays Clay Miner.* **1978**, *26*, 125−134.

(22) Raupach, M.; Emerson, W. W.; Slade, P. G. The arrangement of paraquat bound by vermiculite and montmorillonite. *J. Colloid Interface Sci.* **1979**, *69*, 398−408.

(23) Rodriguez, J. M.; Lopez, A. J.; Bruque, S. Interaction of phenamiphos with montmorillonite. *Clays Clay Miner.* **1988**, *36*, 284−288.

(24) Xu, S.; Boyd, S. A. Cationic surfactant adsorption by swelling and nonswelling layer silicates. *Langmuir* **1995**, *11*, 2508−2514.

(25) Theng, B. K. G.; Aislabie, J.; Fraser, R. Bioavailability of phenanthrene intercalated into an alkylammonium-montmorillonite clay. *Soil Biol. Biochem.* **2001**, *33*, 845−848.

Received for review September 24, 2002. Revised manuscript received February 19, 2003. Accepted February 21, 2003. N.S. was supported by a BOYSCAST Fellowship from the Department of Science and Technology, Government of India. The Remediation of Contaminated Environments Program, CSIRO Land and Water, Australia, funded this work.

JF025978P